In vitro and in silico antioxidant and antimicrobial activity of ethanolic extracts of *Cnidoscolus chayamansa* leaves

Actividad antioxidante y antimicrobiana in vitro e in silico de extractos etanólicos de hojas de *Cnidoscolus chayamansa*

Karla Y. Posada-Mayorga[1]✉ iD, **Jorge Carlos Ruíz-Ruíz**[2]✉ iD, **Zendy Evelyn Olivo-Vidal**[1]✉ iD, **Carlos Alberto Lobato-Tapia**[3]✉ iD, **Neith Aracely Pacheco-López**[4]✉ iD, **Iván Emanuel Herrera-Pool**[4]✉ iD, **Cesar A. Irecta-Najera**[1]✉ iD, and **Xariss M. Sánchez-Chino**[5]*✉ iD

[1] Departamento de Salud, El Colegio de la Frontera Sur-Villahermosa. Carretera a Reforma Km. 15.5 s/n. Ra. Guineo 2da. Sección, Villahermosa, C.P. 86280, Tabasco, México.
[2] Escuela de Nutrición, Universidad Anáhuac Mayab. Carr. Mérida Progreso Km. 15.5. 96 Cordemex, CP. 97310, Mérida, Yucatán, México.
[3] Universidad Politécnica Metropolitana de Puebla, Popocatépetl s/n, Reserva Territorial Atlixcáyotl, Tres Cerritos, 72480 Puebla, Pue., México.
[4] Centro de Investigación y Asistencia en Tecnología y Diseño del Estado de Jalisco A.C. Km 5.5 ca-rretera, Sierra Papacal - Chuburná, C.P. 97302, Chuburná, Yucatán.
[5] CONAHCYT-Departamento de Salud, El Colegio de la Frontera Sur-Villahermosa. Carretera a Reforma Km. 15.5 s/n. Ra. Guineo 2da. Sección, Villahermosa, C.P. 86280, Tabasco.

ABSTRACT

Cnidoscolus chayamansa leaves – used in gastronomy and traditional medicine in Mexico – are rich in phenolic compounds, which may have antioxidant and antimicrobial activity. In this study we evaluated the *in vitro* antioxidant activity and *in silico* antibacterial activity, of ethanolic extracts of *C. chayamansa* leaves obtained by ultrasonication. Phenolic content was 14.37 mg GAE/mL. Guanosine nucleoside and coumaric acid, and kaempferol derivatives were identified through UPLC-PDA-ESI-MS. Evidence of antioxidant activity was demonstrated by the Cu^{2+} chelation activity (65.53 %) and the Fe^{3+} reducing antioxidant power (69.59 %). Although no antibacterial activity was found against *E. coli* and *S. aureus*, the *in silico* analysis revealed that the isolated phenolic compounds modify signaling pathways essential for the survival of the bacteria studied.

Keywords: chaya leaves; phenolic compounds; molecular docking; antioxidant activity; antibacterial activity.

RESUMEN

Las hojas de *Cnidoscolus chayamansa* – utilizadas en la gastronomía y la medicina tradicional en México – son ricas en compuestos fenólicos que pueden tener actividad antioxidante y antimicrobiana. En este estudio evaluamos la actividad antioxidante *in vitro* y la actividad antibacteriana *in silico* de extractos etanólicos de hojas de *C. chayamansa* obtenidos por ultrasonicación. El contenido de compuestos fenólicos fue de 14.37 mg GAE mL^{-1}. Se lograron identificar compuestos como nucleósido de guanosina, ácido cumárico y los derivados de kaempferol mediante UPLC-PDA-ESI-MS. Los extractos tuvieron actividad antioxidante por medio de la quelación del Cu^{2+} (65.53 %) y el poder reductor del Fe^{3+} (69.59 %). Aunque no se encontró actividad antibacteriana contra *E. coli* y *S. aureus*, por medio de la inhibición de creci-miento en disco, el análisis *in silico* reveló que los compuestos fenólicos aislados modifican las vías de señalización esencia-les para la supervivencia de las bacterias estudiadas.

Palabras clave: hojas de chaya; compuestos fenólicos; docking molecular; actividad antioxidante; actividad antibacte-riana.

INTRODUCTION

Cnidoscolus chayamansa, commonly known as *chaya* is an endemic shrub of Tabasco and the Yucatan Peninsula in Mexico (Pérez-González *et al*., 2019) used in local gastronomy, in addition to traditional medicine (Rodrigues *et al*., 2021) presumably due to a high content of bioactive compounds (phenols, flavonoids, coumarins, and cyanogenic glycosides) in its leaves (Gutiérrez-Rebolledo *et al*., 2016; Bautista-Robles *et al*., 2020). The antioxidant activity of bioactive compounds plays a fundamental role through multiple pathways, preventing oxidative stress (OS)-related diseases (Pisoschi *et al*., 2021) such as diabetes mellitus and cardiovascular diseases (scavenging free radicals, increasing the activity of endogenous antioxidant enzymes, improvement of insulin resistance and enhancement of glucose uptake and metabolism) (Huang *et al*., 2020; Garcia and Blesso, 2021), as well as cancer, they induce apoptosis, by lowering the nucleoside diphosphate kinase-B activity (involved in nucleic acid replication), inhibiting cell-proliferation and cell cycle arrest by suppressing the NF-kB pathway in various cancers (Hazafa *et al*., 2020).

OS occurs when reactive oxygen species (ROS) and free radicals (FR) increase, which may cause cellular and tissue damage (Ouadi *et al*., 2017). Bioactive compounds such as polyphenols may act as antioxidants, anti-inflammatory, and antimicrobial agents through modulation of inhibitory re-

ceptors of inflammation and activators of anti-inflammatory enzymes (Kaabi, 2022).

A positive correlation exists between the content of phenolic compounds and the antibacterial capacity, including bacteriostatic and bactericidal properties. Phenolic compounds modify the bacterial cytoplasmic membrane permeability and inhibit signaling pathways involved in bacterial survival (Vazquez-Armenta *et al*., 2022). Research shows that ethanolic extracts of *C. chayamansa* leaves showed high antibacterial activity against *S. aureus*, *B. Cereus*, *E. coli*, *K. pneumo*niae and *S. pyogenes* (Elizabeth *et al*., 2023). Moreover, the extraction method can affect the concentration of phenolic compounds; for instance, modern extraction methods based on sonication – generated through the coupling of high-power and low-frequency ultrasound waves that travel through the liquid medium, causing cycles of low and high-pressure and creating acoustic cavitation bubbles that collapse releasing a large number of compounds present in the sample (Chemat *et al*., 2017; Fu *et al*., 2020). The current study aimed to evaluate the *in vitro* and *in silico* antioxidant and antibacterial potential of the Ultrasonic Assisted Ethanolic Extracts (UAEE) of *C. chayamansa* leaves.

MATERIALS AND METHODS

Collection and preparation of samples. Leaves of *C. chayamansa* were collected on February 2022, from the edge of the Teapa River (17°33'49.3"N 92°57'09.7"W), Joyas del Pedregal, in the municipality of Teapa, Tabasco, Mexico, and studied in the herbarium from El Colegio de la Frontera Sur (code HET 2459, HET 2460, and HET 2461). Leaves were washed with drinking water, dried in a dehydrator (Model 32 100, Hamilton Beach) at a constant temperature of 41 °C for 18 hours, and grounded until pulverized.

Ultrasonic Assisted Ethanolic Extracts (UAEE)
The ethanolic extraction comprised 10 g of dry leaves of *C. chayamansa* in 100 mL of aqueous ethanol (1:1) using a 40 kHz ultrasonic mechanical bath (1800, Branson, St. Louis, MO, USA) at 25 °C for 30 min. The extracts were filtered through Whatman #1 paper (150 mm diameter) and stored at 4 °C (Pérez-González *et al*., 2019).

Quantification and profile of phenolic compounds from Ultrasonic Assisted Ethanolic Extracts (UAEE)
The Folin-Ciocalteu method (Ruiz *et al*., 2015) was used to estimate the concentration of phenolic compounds from *C. chayamansa*, with gallic acid as the standard (≥ 98.0, CAS: 5995-86-8, Fermont, Monterrey, Mexico). The analyses were carried out in triplicate, and results are expressed as mg of Gallic Acid Equivalents (mg GAE/mL).

The profile of phenolic compounds from Ultrasonic Assisted Ethanolic Extracts (UAEE) of *C. chayamansa* was determined through ultra-performance liquid chromatography coupled with a photodiode array detector and electrospray ionization mass spectrometry (UPLC-PDA-ESI-MS); using an ultra-performance liquid chromatograph (UPLC) (ACQUITY UPLC H-Class, Waters Corporation, Milford, MA, USA) equipped with a quaternary pump (UPQSM), and an automatic injector (UPPDALTC). Chromatographic separation was performed on a Waters' ACQUITY UPLC BEH C18 column, 1.7 μm, 100 x 2.1 mm I.D (Milford, MA, USA) under similar conditions reported by Herrera-Pool *et al*. (2021). The Photodiode Array Detector (PDA) was set to scan within a wavelength (λ) range from 190 nm to 600 nm. The absorbance response was taken from channels A (290 nm) and B (350 nm). Mass spectra (Xevo TQ-S Micro, Waters, Chicago, IL, USA) were recorded in full scan negative ion mode at 50 - 2000 m/z. Compounds were identified by comparing the observed spectral fingerprint data with those reported in Pubchem and MassBank databases.

Determination of antioxidant activities *in vitro*
Chelating capacity of Cu^{2+} and Fe^{2+} *in vitro*
Chelating activity of Cu^{2+} was determined with the method reported by Saiga *et al*. (2003), mixing 250 μL of sodium acetate buffer (50 mM, pH 6.0) with 250 μL of 20 mM Cu^{2+} standard solution and 25 μL of 0.1 % violet pyrocatechol, reacted for 5 min at 25 °C and then 250 μL of the blank (distilled water) or UAEE samples were added. The absorbances were measured at 632 nm in a spectrophotometer (VE-5100UV, Velab, Pharr, TX, USA). All samples were performed in triplicate. The copper chelating activity was calculated as:

$$\% \ CC \ Cu^{2+} = (\text{Sampler Abs - Blank Abs})/(\text{Sampler Abs}) \times 100 \quad \text{(Eq 1)}$$

Where % CC Cu^{2+} represents the percentage of copper chelated.

The Fe^{2+} chelating capacity was determined by the method used by Ruiz *et al*. (2015). Briefly, the absorbance of a blank and the UAEE samples were read, mixing 250 μL of sodium acetate buffer (100 mM, pH 4.9) with 250 μL of 20 mM Fe^{2+} standard solution, and 250 μL of water (in the case of the blank) or 250 μL of UAEE. Next, it was left to react for 5 min at room temperature and then 50 μL of 40 mM ferroxine solution were added. Absorbances were measured at 562 nm in a spectrophotometer (VE-5100UV, Velab, Pharr, TX, USA). All samples were processed in triplicate. The Fe^{2+} chelating activity is estimated as shown in Eq. 2:

$$\% \ CC \ Fe^{2+} = (\text{Sampler Abs-Blank Abs})/(\text{Blank Abs}) \times 100 \quad \text{(Eq 2)}$$

Where % CC Fe^{2+} represents the percentage chelating capacity.

Fe^{3+} reducing power
The Fe^{3+} reducing power was determined using the method described by Sudha *et al*. (2011). Briefly, absorbance measurements from a blank (distilled water) and UAEE were made. 250 μL of blank or sample were taken and 250 μL of phosphate buffer (0.2M, pH 6.6) and 250 μL of 1 % $K_3[Fe(CN)_6]$ were added in each case, shaken for 5 sec in a vortex and

incubated at 50 ºC for 20 min. Once the incubation was completed, 250 µL of 10 % $C_2HCl_3O_2$ was added, 500 µL of this mixture was taken and deposited in a 2 mL Eppendorf tube, and then 400 µL of distilled water and 100 µL of 0.1% $FeCl_3$ were added, mixed for 5 seconds in a vortex and incubated at 50 ºC for 10 minutes. Finally, the samples were centrifuged at 3000 rpm for 10 min in a centrifuge with a 10 cm rotor diameter (J-40, Solbat. Edo. Mex., Mexico), and the absorbances of the supernatant were read at 700 nm in a spectrophotometer (VE-5100UV, Velab, Pharr, TX, USA). All samples were analyzed in triplicate. The Fe^{3+} reducing power was estimated as shown in Eq 3:

% PR Fe^{2+} = (Sampler Abs-Blank Abs)/(Sampler Abs)×100   (Eq. 3)

Where % PR Fe^{2+} represents the percentage reducing power of Fe^{3+}.

ABTS radical scavenging capacity

ABTS radical scavenging capacity was determined by the method reported by Ruiz *et al*. (2015) with some modifications. First, a 2.0 mM ABTS solution was prepared, then the $ABTS^+$ radical cation was produced with a 70 mM $K_2S_2O_8$ solution, allowing the mixture to remain in the dark at 25 ºC for 16 hours before use. Subsequently, this solution was diluted with phosphate buffer (1.0 M, pH 7.4) until obtaining an absorbance of 0.800 ± 0.030 at 734 nm. Next, 10 µL of UAEE diluted 1:10 were taken and reacted with 990 µL of the $ABTS^+$ radical diluted in phosphate buffer. Next, the absorbance at 734 nm was measured in a spectrophotometer (VE-5100UV, Velab, Pharr, TX, USA) after 1 and 6 min of reaction. The same procedure was performed with a blank sample using 50% ethanol. All samples were analyzed in triplicate. The $ABTS^+$ radical scavenging percentage (% RS) of the samples were calculated as shown in Eq. 4:

% RS = (Sampler Abs-Blank Abs)/(Sampler Abs)×100   (Eq. 4)

Where % RS represents the percentage ABTS radical scavenging.

DPPH radical scavenging capacity

The DPPH radical scavenging capacity was done according to the method proposed by Fukumoto and Mazza (2000), with some modifications. Briefly, a 0.1 mM DPPH solution in ethanol was prepared. UAEE samples diluted 1:10 and distilled water (as a blank) were analyzed. The procedure was the same for both. 100 µL of blank and 100 µL of extracts were taken individually and 1000 µL of the DPPH solution were added to each one, then shaked in a vortex for 10 seconds and allowed to react for 30 minutes in the dark. Next, their absorbances were read at 517 nm in a spectrophotometer (VE-5100UV, Velab, Pharr, TX, USA). All samples were analyzed in triplicate. The % uptake of RL DPPH was determined as shown in Eq. 5:

% RSC = (Sampler Abs-Blank Abs)/(Sampler Abs)×100   (Eq. 5)

Where % RSC represents the percentage DPPH radical scavenging capacity.

Fe^{3+} reducing power

The reducing power of Fe^{3+} was determined using the method described by Sudha *et al*. (2011). Briefly, absorbance measurements from a blank (distilled water) and UAEE of *C. chayamansa* were made. 250 µL of blank or sample were taken, mixed with 250 µL of phosphate buffer (0.2M, pH 6.6) and 250 µL of 1% $K_3[Fe(CN)_6]$ in each case, shaken for 5 seconds in a vortex and incubated at 50 ºC for 20 minutes. Once the incubation was completed, 250 µL of 10 % $C_2HCl_3O_2$ were added, then 500 µL of this mixture were taken and deposited in a 2 mL Eppendorf tube, 400 µL of distilled water and 100 µL of 0.1% $FeCl_3$ were added, mixed for 5 seconds in a vortex and incubated at 50 ºC for 10 min. Finally, the samples were centrifuged at 3000 rpm for 10 min in a centrifuge with a 10 cm rotor diameter (J-40, Solbat. Edo. Mex., Mexico, and the absorbances of the supernatant measured read at 700 nm in a spectrophotometer (VE-5100UV, Velab, Pharr, TX, USA). All samples were analyzed in triplicate. The reducing power of Fe^{3+} was estimated as shown in Eq. 3:

% PR Fe^{2+} = (Sampler Abs-Blank Abs)/(Sampler Abs)×100   (Eq. 3)

Where % PR Fe^{2+} represents the percentage reducing power of Fe^{3+}.

Antibacterial activity

The antibacterial activity of the UAEE of *C. chayamansa* was evaluated against *Escherichia coli* (G- ATCC 25922) and *Staphylococcus aureus* (G+ ATCC 25923). The agar disc diffusion method was performed on Muller-Hilton agar (MCD LAB, Cat 7131, Mex), prepared according to the manufacturer's specifications and sterilized in an autoclave at 1.055 Kgf/cm² for 15 min. After that, 30 mL of agar were distributed in Petri dishes which were impregnated with 100 µL per box with the adjusted suspension of each indicator bacteria. Six-mm diameter sterile discs were impregnated with 30 µL of UAEE. As a positive control antibiogram discs were used with amoxicillin and clavulanic acid (AMC) at a concentration of 30 µg/mL. As negative controls, disks impregnated with 30 µL of sterilized water were used. All samples were analyzed in triplicate for each type of extract and were incubated at 37 °C for 24 h. Growth inhibition halos were measured with a Vernier Calliper (Calliper, Lenfech, 0 mm - 150 mm measuring range). The antibacterial activity was assessed according to Capitani *et al*. (2016) parameters.

In silico antibacterial activity

For *in silico* antibacterial activity, the crystal structure of key receptors for *E. coli* (2WUB, 4XO8) and *S. aureus* (2W9S, 2ZCO) were retrieved from the Protein Data Bank (http://www.rcsb.org/

). The structures were prepared using the Dock Prep Module of UCSF Chimera 1.14 (Pettersen *et al.*, 2004) by removing water molecules, sidechains and ligands, adding hydrogens, and assigning partial charges. However, the Mg ion was kept due to its importance for the 4WUB protein function. Protein fragments were reconstructed by applying SWISS-MODEL (Waterhouse *et al.*, 2018).

Ligands – Guanosine, Kaempferol-3-O-rutinoside, Kaempferol-3-(2G-glucosylrutinoside)-7-rhamninoside, Kaempferol-3-O-rhamninoside, Kaempferol-3-(2G-glucosylrutinoside) and Rutin – and control compounds (trimethoprim, farnesyl thiopyrofosfate, heptyl-α-D-mannopyrannoside, and phosphoaminophosphoric acid adenilate ester) were retrieved in Mole2 file format (.mol2) from PubChem (https://pubchem.ncbi.nlm.nih.gov/). Avogadro 1.2.0 (Hanwell *et al.*, 2012) optimized f ligands' molecular geometry and converted the input files to .pdb files, later prepared using the Chimera docking tool.

All structures were aligned on a grid box large enough to accommodate all the experimental ligands used for molecular docking analysis. The grid size and the grid box coordinates for each target were as follows: 2WUB, 25×25×25 Å (14.57, 19.81, -10.80); 4OX8, 30×30×30 Å (-43.84, 5.15, 3.86); 2W9S, 25×25×25 Å (2.67, -2.13, 44.93); and 2ZCO, 30×30×30 Å (53.86, 10.35, 51.81). Ten independent docking runs were executed for each structure with the Autodock Vina tool

(Eberhardt *et al.*, 2021). Additionally, ten replicates were performed for each combination of ligand and receptor, which were analyzed through LigPlot+ (Laskowski *et al.*, 2011) and PyMOL (De Lano *et al.*, 2002).

Docking results were validated by extracting the co-crystallised ligands of the 2W9S, 2ZCO, 4XO8, and 4WUB proteins and re-docking them into the same position. The ligands pose with the lowest energy obtained on re-docking, and the co-crystallised ligands were superimposed to calculate the RMSD values in PyMOL software. The RMSD values must be within a reliable range of 2 Å to validate the docking process (Jug *et al.*, 2015). Table 1 summarizes the binding affinity between the *C. chayamansa* compounds, bacterial proteins, and ligand-amino acid interactions.

Statistical analysis
Results were summarized by descriptive statistics using R Studio (V 4.2.1) and reported as mean ± standard error of the mean.

RESULTS AND DISCUSSION
Phenolic compounds in ethanolic extracts of *C. chayamansa*
The concentration of phenolic compounds in the UAEE of *C. chayamansa* leaves was 143.7 mg of gallic acid equivalents

Table 1. Binding affinities between *C. chayamansa* compounds and bacterial proteins and ligand-amino acid interactions.
Tabla 1. Afinidades de unión entre compuestos de *C. chayamansa* y proteínas bacterianas e interacciones ligando-aminoácido.

Target	Ligand	Binding affinities (Kcal/mol)	Amino acid interactions
2W9S	Guanosine	-8.0	I14, G15, N18, Q19, K45, T46, I50, G94, Y98, T121
	Kaempferol-3-O-rutinoside	-9.5	I5, A7, L20, W22, H23, D27, L28, T46, I50, F92, Y98
	Kaempferol-3-(2G-glucosylrutinoside)-7-rhamninoside	-7.7	A7, L20, H23, I31, L32, T46, I50, L52, R57, F92, Y98
	Kaempferol-3-O-rhamninoside	-9.3	A7, Q19, L20, L28, I31, T46, I50, F92, Y98
	Kaempferol-3-(2G-glucosylrutinoside)	-7.7	I5, A7, Q19, L20, T46, I50, L52, F92, Y98
	Rutin	-9.2	A7, L20, W22, H23, D27, T46, S49, I50, F92, G94, Y98
	Trimethoprim	**-7.6**	A7, I14, G46, N18, L20, D27, I31, T46, S49, F92, Y98, T121
2ZCO	Guanosine	-7.4	N17, H18, R45, D48, Q165, N168, D172, Y183, R265
	Kaempferol-3-O-rutinoside	-10.1	H18, R45, D48, Y129, Q165, V133, I169, D172, Y183
	Kaempferol-3-(2G-glucosylrutinoside)-7-rhamninoside	-10.4	D49, D52, V111, D114, Q165, N168, N179, R181, D172, D176, R265
	Kaempferol-3-O-rhamninoside	-9.3	H18, Y41, R45, D49, D114, Y129, D172, R181, Y183
	Kaempferol-3-(2G-glucosylrutinoside)	-8.9	R45, D48, D49, V111, D114, Q165, D172, D176, R181, Y183
	Rutin	-9.8	D48, V111, D114, Y129, V133, Q165, N168, D176, R181, Y183
	Farnesyl thiopyrophosphate	**-7.2**	H18, F22, Y41, R45, A134, A157, L160, Q165, N168, R171, D172
4XO8	Guanosine	-6.6	F1, D46, D47, Y48, I52, D54, Q133, N135, D140, F142
	Kaempferol-3-O-rutinoside	-6.9	D37, L76, S78, G79, V93, V94, Y95, L101, P102, P104, V105
	Kaempferol-3-(2G-glucosylrutinoside)-7-rhamninoside	-5.9	A2, C3, L4, G8, A10, P12, F43, H45, D47, R98, D100
	Kaempferol-3-O-rhamninoside	-6.9	F1, P12, H45, N46, D47, Y48, D54, R98, Q133, N135, D140, F142
	Kaempferol-3-(2G-glucosylrutinoside)	-6.1	A2, C3, A10, I13, P12, F43, H45, D47, R98, T99, D100
	Rutin	-6.8	D37, L76, S79, G79, V93, V94, Y95, L101, P102, P104
	Heptyl-α-D-mannopyranoside	**-6.5**	F1, I13, N46, D47, Y48, I52, D54, Q133, N135, D140,
4WUB	Guanosine	-8.3	N46, E50, D73, G77, I78, P79, I94, L103, Y109, V120, T165
	Kaempferol-3-O-rutinoside	-9.2	N46, A90, V93, I94, G101, G102, L103, D105, N107, S108, Y109
	Kaempferol-3-(2G-glucosylrutinoside)-7-rhamninoside	-8.7	E50, I78, H83, V93, G101, G102, D105, N107, Y109, R136
	Kaempferol-3-O-rhamninoside	-8.9	N46, E50, R76, P79, H83, I94, G101, G102, D105, N107, S108, Y108
	Kaempferol-3-(2G-glucosylrutinoside)	-8.5	P79, H83, A90, G101, G102, L103, D105, N107, S108, Y109, R136
	Rutin	-10.1	E50, D73, P79, H83, I94, G101, G102, L103, S108, Y109, G117
	Phosphoaminophosphoric acid adenylate ester	**-11.1**	N46, D73, V97, A100, G102, L103, L115, H116, G117, V118, G119, V120, S121, Q335, L337

(mg GAE)/g dry leaves. Guanosine nucleoside and different coumaric acid and kaempferol derivatives were identified (Table 2). Other compounds reported in extracts of *C. chaya-mansa* leaves are rutin, naringenin, chlorogenic acid, ferulic acid, protocatechuic acid, astragalin, caffeic acid, myristic acid, riboflavin, and β-carotene (Guzmán *et al*., 2020). Kaempferol has an antioxidant activity via free radical elimination (Hussain *et al*., 2021), coumaric acid (a hydroxycinnamic acid, i.e. a hydroxy metabolite cinnamic acid) has a high antibacterial, antioxidant, and anti-inflammatory potential related to the prevention of cardiovascular diseases (Liu *et al*., 2020).

In a study where the effect of the aqueous extract of chaya leaves (*Cnidoscolus aconitifolius*) in precarcinogenic lesions was evaluated, a minor concentration of total phenolic compounds (52.5 mg galic acid equivalents/g of dry leaf) was reported, which differs from our results. The presence of p-coumaric acid is reported, which together with rosmarinic acid, chlorogenic acid, resveratrol and luteoin are the major compounds in extracts obtained; other compounds identified were gallic acid, caffeic acid, vanilic acid, vanillin, resveratrol, apigenin y ferulic acid (Kuri-García *et al*., 2019).

Us-Medina *et al*. (2020) evaluated the *in vitro* antioxidant and anti-inflammatory activity of biologically active compounds from *C. aconitifolius* extracts, reporting a greater amount of phenolic compounds in aqueous extracts (706.1 mg galic acid equivalents/g of dry leaf) than those reported here; for ethanolic extracts, 351.3 mg galic acid equivalents/g of dry leaf were also reported in *C. aconitifolius* aqueous extracts. The concentration of phenolic compounds may vary according to the solvent used. Polar solvents are employed for plant extractions since they contain bonds between atoms that differ in electronegativity (e.g., O-H) and form hydrogen bonds; therefore, they are suitable for dissolving polar reactants such as ions (Li *et al*., 2018). Ethanol has a lower polarity than methanol, however, ethanol is Generally Recognized as Safe (GRAS) by the Food and Drug Administration (FDA).

In vitro antioxidant activity
The antioxidant potential of natural extracts is associated with the content of phenolic compounds. The main antioxidant potential of the UAEE of *C. chayamansa* leaves was obtained in the Cu^{2+} chelation activity assays (65. 53 ± 1.72)

Table 2. Phenolic compounds detected in Ultrasonic Assisted Ethanolic Extracts (UAEE). The identified compounds that showed a higher signal intensity are shown in bold.
Tabla 2. Compuestos fenólicos detectados en Extractos Etanólicos Asistidos por Ultrasonido (UAEE). Los compuestos identificados que mostraron una mayor intensidad de señal se muestran en negrita.

Peak #	RT (PDA detector)	λ max	Molecular ion ([M – H]⁻) m/z	Fragments m/z	Tentative identification
1	6.93	253, 280sh	282	150	*Guanosine*
2	8.26	198, 266, 317	901	755, 593, 447, 355, 283	*Kaempferol 3-(2G-glucosylrutinoside)-7-rhamnoside*
3	8.39	221, 280sh, 311	355	209, 191, 147, 85	*Coumaroyl aldaric acid (Isomer I)*
4	8.45	197, 290sh, 312	355	209, 191, 147, 85	*Coumaroyl aldaric acid (Isomer II)*
5	8.64	221, 295sh, 311	355	209, 191, 147, 85	*Coumaroyl aldaric acid (Isomer III)*
6	8.69	210, 290sh, 316	355	209, 191, 147, 85	*Coumaroyl aldaric acid (Isomer IV)*
7	8.86	196, 300	355	209, 191, 147, 85	*Coumaroyl aldaric acid (Isomer V)*
8	8.95	197, 290sh, 312	355	209, 191, 147, 85	*Coumaroyl aldaric acid (Isomer VI)*
9	9.11	195, 262sh, 310	355	209, 191, 147, 85	*Coumaroyl aldaric acid (Isomer VII)*
10	9.25	197, 254, 268sh, 343	755	300, 284	*Kaempferol 3-(2G-glucosylrutinoside)*
11	**9.57**	**210, 265, 346**	**739**	**284, 254, 227**	***Kaempferol 3-O-rhamninoside***
12	9.72	203, 255, 268sh, 352	609	300, 271	*Rutin*
13	**10.17**	**210, 265, 343**	**593**	**284, 254, 227**	***Kaempferol-3-O-rutinoside (Isomer I)***
14	**10.29**	**210, 265, 348**	**593**	**284, 254, 227**	***Kaempferol-3-O-rutinoside (Isomer II)***
15	10.56	195, 266, 307	593	284, 254, 227	*Kaempferol-3-O-rutinoside (Isomer III)*
16	10.90	197, 265, 344	593	284, 254, 227	*Kaempferol-3-O-rutinoside (Isomer IV)*
17	11.22	210, 265, 321	447	284, 254, 227	*Kaempferol-3-O-hexoside (Isomer I)*
18	11.66	197, 265, 346	447	284, 254, 227	*Kaempferol-3-O-hexoside (Isomer II)*

RT: Retention time

and Fe^{3+} reducing power (69.59 %). Regarding the ABTS and DPPH free radical trapping capacity, the antioxidant potential was less than 50 % (37.74 ±3.43 and 14.24± 0.22% respectively), and the Fe^{2+} chelation activity was 15.71 ± 0.82%. However, the antioxidant activity by the DPPH method was higher than that reported by García-Rodríguez *et al*. (2013), which was 10.66% in ethanolic extract of *C. chayamansa*, and 254.04 µmol Fe^{2+}/L for assay of ferric reducing power; this extract contained 35.7 mgEAG/g of leaf; the authors reported the presence of, coumarins, flavonoids, lignans and cyangenic glycosides. Among their findings, the authors reported that the ethanolic extracts of *C. chayamansa* also had anti-inflammatory activity in the *in vivo* model, although it was low, which was related to the concentration of phenolic compounds.

Antioxidant activity has also been reported in other species of the genus *Cnidoscolus*, although by other methods such as TEAC and ORAC, with values of 539 and 926 µmol Trolox equivalents/g of lyophilized extract respectively, in ethanolic extracts of *C. aconitifolius* leaf. These extracts had phenolic compounds (52.5 mg GAE/g) and flavonoids (41.6 mg catechin equivalent/g); the administration of these extracts in experimental animals protected against colon cancer in a model in which an oxidizing agent (azoxymethane) and an inflammatory agent (dextran sodium sulfate), through inhibiting cell proliferation and inflammation of colonic lesions by decreasing β-catenin and at long-term COX-2 reduction, although a high expression of NF-jB (Kuri-García *et al*., 2019).

In vitro and *in silico* antibacterial activity

For *in vitro* antibacterial activity assay, the inhibition halos in positive controls showed high activity against Gram-negative and Gram-positive bacteria strains (Table 3). Conversely, the halos of inhibition size in UAEE of *C. chayamansa* leaves was less than 10 mm, hence, considered inactive (Capitani *et al*., 2016). This could have been mainly due to the solvent or extract concentration used, other authors reported that ethanol extract of *C. chayamansa* leaves contained flavonoids, saponins, cardenolides and polyphenols with antibacterial activity against *S. aureus*, with an inhibition zone of 13.2 mm, greater than that found in this study (9.96 mm). Also, for the test in *E. coli* the activity was greater (14.83 mm) than that

Table 3. Antibacterial activity of Ultrasonic Assisted Ethanolic Extracts (UAEE) from *C. chayamansa* leaves.

Tabla 3. Actividad antibacteriana de extractos etanólicos obtenidos por ultrasonicación (UAEE) de hojas de *C. chayamansa*.

	Escherichia coli	*Staphylococcus aureus*
UAEE	7.90*	9.96*
AMC	20.05****	42.93****
C-	7.28*	6.46*

UAEE: Ultrasonic Assisted Ethanolic Extract, AMC: amoxicillin with clavulanic acid C+; positive control)y C-: negative control *inactive, ** partially active, ***active **** very active (Capitani *et al*., 2016).

UAEE: Extracción Etanólica Asistida por Ultrasonido; AMC: Amoxicilina con ácido clavulánico; C+ Control positivo; C- Control negativo; *inactivo, ** parcialmente activo, ***activo y **** muy activo (Capitani *et al*., 2016).

reported by us (7.9 mm). On the other hand, they demonstrated that *C. chayamansa* extracts obtained with different solvents had activity agains Gram-positive pathogenic bacteria (*B. Cereus* and *S. pyogenes*) and Gram negative pathogenic bacteria (*E. coli* and *K. pneumoniae*), using ciprofloxacin as a control (Elizabeth *et al*., 2023).

For *in silico* assays, target proteins can be proposed for future tests, either *in vitro* or *in vivo*, in this sense, target proteins involved in the viability of *S. aureus* were selected for antibacterial potential evaluation of the extracted compounds against these microorganisms (Figure 1). Firstly, Dihydrofolate Reductase (DHFR, 2W9S) (https://www.rcsb.org/structure/2w9s) involved in the folic acid pathway in *S. aureus*, which promotes thymidylate biosynthesis essential for cell replication and proliferation (He *et al*., 2020; Bourne *et al*., 2010). Secondly, Dehydrosqualene Synthase (CrtM, 2ZCO) (https://www.rcsb.org/structure/2ZCO) responsible for synthesizing the golden carotenoid pigment staphyloxanthin of *S. aureus*, which provides its antioxidant properties, aiding bacteria survival within the host cell (Kahlon *et al*., 2010; Wu *et al*., 2019). Inhibitors targeting DHFR and CrtM potentially induce bacterial death and serve as effective targets for treating bacterial infections.

Molecular docking was conducted to determine the target protein–compound binding energy. All six characterized compounds were docked against 2W9S and 2ZCO proteins using Autodock Vina. Almost all the evaluated ligands showed higher affinities than the co-crystallized ligands found in the crystal structures of each target during re-docking. The most favorable ligand-target complexes were Kaempferol-3-O-rutinoside-2W9S (-9.5 kcal/mol) and Kaempferol-3-(2G-glucosylrutinoside)-7-rhamninoside-2ZCO (-10.4 kcal/mol).

Two targets from *E. coli* were selected to evaluate the inhibitory potential of the compounds identified through the UAEE of *C. chayamansa* leaves. The first target is the FimH protein (4XO8), a bacterial adhesion lectin located at the tip of *E. coli* type 1 fimbriae or pili. These structures facilitate bacterial binding to surfaces that display mannose residues (Hartmann et al., 2011; Magala et al., 2020). The second target is the DNA gyrase B subunit (4WUB), which plays a crucial role in regulating the physiological function of the genome and providing the energy required for DNA supercoiling (Sissi et al., 2010). This enzyme is an ideal target for antibacterial drugs due to its potential for selective toxicity (Sissi *et al*., 2010; Fois *et al*., 2020).

Molecular docking evaluated the binding energy between the 4XO8 and 4WUB proteins, and the six compounds through Autodock Vina. The evaluated ligands showed similar affinities to the co-crystallized ligands, particularly with 4XO8. However, for 4WUB, the evaluated ligands exhibited slightly lower activity compared to the co-crystallized ligand, Phosphoaminophosphoric acid adenylate ester. The most favorable ligand-target complexes were Kaempferol-3-O-rutinoside-4XO8 (-6.9 kcal/mol) and Rutin-4WUB (-10.1 kcal/mol).
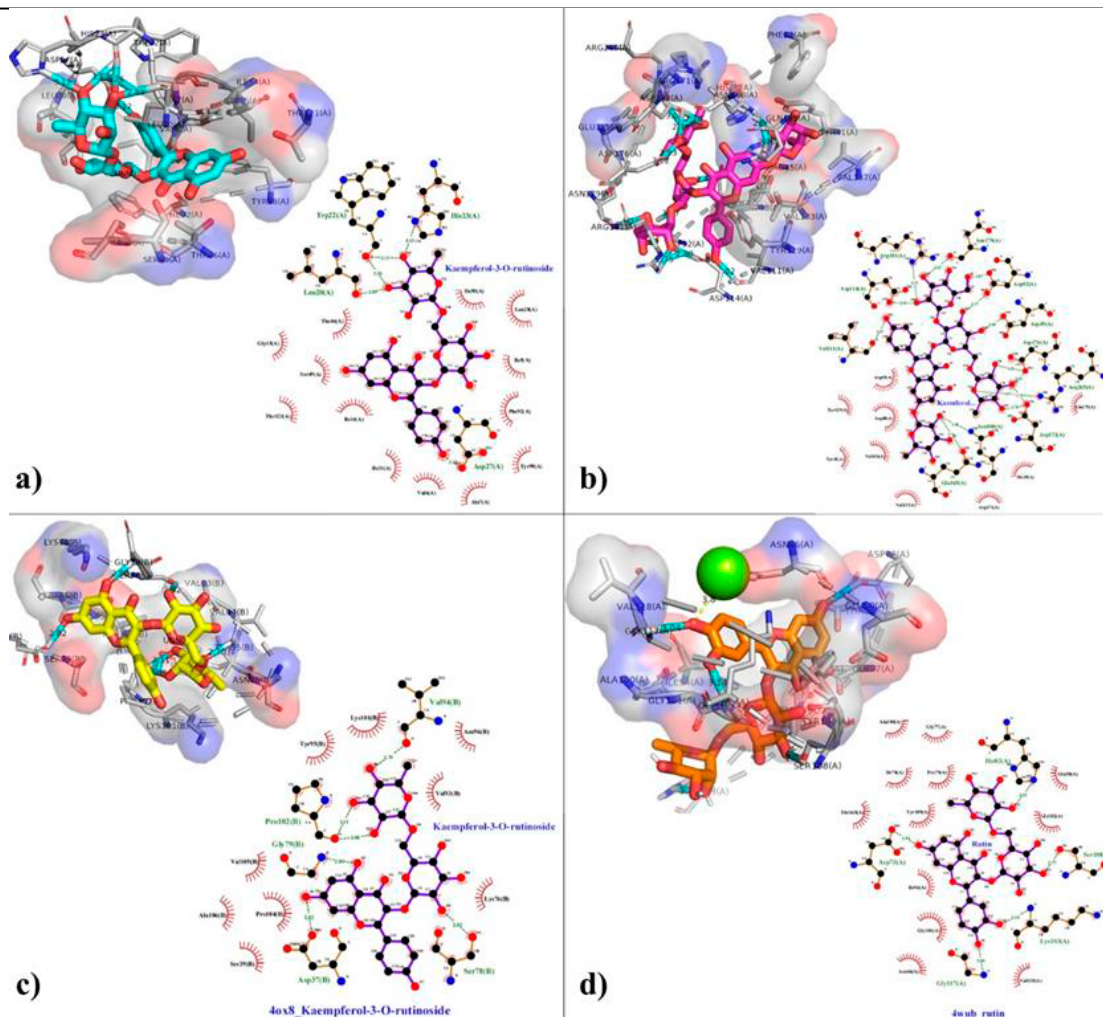
Figure 1. Two and three-dimensional representation of the hydrogen bonding and hydrophobic interaction between ligands within the binding cavity of receptors. a) Kaempferol-3-O-rutinoside-2W9S complex, b) Kaempferol-3-(2G-glucosylrutinoside)-7-rhamni-noside-2ZCO complex, c) Kaempferol-3-O-rutinoside-4OX8 complex and d) Rutin-4WUB complex.
Figura 1. Representación bidimensional y tridimensional de los enlaces de hidrógeno y la interacción hidrofóbica entre ligandos dentro de la cavidad de unión de los receptores. a) Complejo Kaempferol-3-O-rutinósido-2W9S, b) Complejo Kaempfe-rol-3-(2G-glucosilrutinósido)-7-ramninósido-2ZCO, c) Complejo Kaempfe-rol-3-O-rutinósido-4OX8 y d) Rutin-4WUB complejo.

Due of the results obtained, it´s possible that the compounds from the *C. chayamansa* extract could exert a bacteriostatic effect on *E. coli* cultures during the *in vitro* antibacterial activity evaluation via inhibition of 4WUB, explaining the observed inhibition halos, such as Tang *et al*. (2022) and Biasi-Garbin *et al*. (2022) obtained with similar methodologies. On the other hand, 4XO8 inhibition was unclear in the *in vitro* evaluation; however, it suggests that the evaluated compounds can bind to these lectins, thereby obstructing bacterial adhesion to host tissues.

CONCLUSIONS
The compounds present in UAEE from *C. chayamansa* leaves, are guanosine nucleoside and different coumaric acid and kaempferol derivatives. These compounds could be related to Cu^{2+} chelation activity and Fe^{3+} reducing antioxidant power. Although the antibacterial activity is not conclusive in the inhibition halos assays, the molecular docking results

suggest that the identified compounds could intervene in metabolic processes necessary for the survival and replication of *E. coli* and *S. aureus*. Therefore, subsequent studies are necessary to evaluate the effect of different concentrations of *C. chayamansa* leaves extracts and their isolated compounds on bacterial strains.

CONFLICTS OF INTEREST
The authors declare no conflict of interest.

REFERENCES

Bautista-Robles, V., Guerrero-Reyes, G., Sánchez-Torres, G.I., Parada-Luna, F., Barrios-Gutiérrez, J.J., Vázquez-Cerero, D., Martínez-Sala, G., Siliceo-Murrieta, J.I., González-Villoria, R.A.M., and Keita, H. 2020. *Cnidoscolus aconitifolius*: therapeutic use and phytochemical properties. Literature review. Revista de la Facultad de Medicina. 68(3):446-452. doi: 10.15446/revfacmed.v68n3.75184

Belabdelli, F., Bekhti, N., Piras, A., Benhafsa, FM., Ilham, M., Adil, S., and Anes, L. 2022. Chemical composition, antioxidant and antibacterial activity of *Crataegus monogyna* leaves extracts. Natural Products Research. 36(12):3234-3239. doi: 10.1080/14786419.2021.1958215

Biasi-Garbin, R.P., Fabris, M., Morguette, A.E.B., Andriani, G.M., Cabral, W.R., Pereira, P.M., Brito, T.O., Macedo Jr, F., Da Silva-Lima, C.H., Nakamura, C.V., Pinge-Filho, P., Tavares, E.R., Yamauchi L.M., Bispo, M.L.F., and Yamada-Ogatta, S.F. 2022. In vitro antimicrobial screening of benzoylthioureas: Synthesis, antibacterial activity toward *Streptococcus agalactiae* and molecular docking study. ChemistrySelect, 7(34), e202202117. doi: 10.1002/slct.202202117

Bourne, C.R., Barrow, E.W., Bunce, R.A., Bourne, P.C., Berlin, K.D., and Barrow, W.W. 2010. Inhibition of antibiotic-resistant *Staphylococcus aureus* by the broad-spectrum dihydrofolate reductase inhibitor RAB1. Antimicrobial Agents and Chemotherapy. 54(9): 3825-3833. doi: 10.1128/AAC.00361-10

Capitani, M.I., Matus-Basto, A., Ruiz-Ruiz, J.C., Santiago-García, J.L., Betancur-Ancona, D.A., Nolasco, S.M., Tomás, M.C., and Segura-Campos, M.R. 2016. Characterization of biodegradable films based on *Salvia hispanica* L. protein and mucilage. Food Bioprocess Technology. 9(8):1276-1286. doi: 10.1007/s11947-016-1717-y

Chemat, F., Rombaut, N., Sicaire, A.G., Meullemiestre, A., Fabiano-Tixier, A.S., and Abert-Vian, M. 2017. Ultrasound assisted extraction of food and natural products. Mechanisms, techniques, combinations, protocols and applications. A review. Ultrasonics Sonochemistry. 34:540-560. doi: 10.1016/j.ultsonch.2016.06.035

De Lano, W.L. 2002. Pymol: an open-source molecular graphics tool, CCP4 Newsletter. On Protein Crystallography. 40:82-92.

Eberhardt, J., Santos-Martins, D., Tillack, A., and Forli, S. 2021. AutoDock Vina 1.2.0: New docking methods, expanded force field, and python bindings. Journal of Chemical Information and Modeling. 3891-3898, 61(8). doi: 10.1021/acs.jcim.1c00203

Elizabeth, H., Channamma, G.M., Gnanasekaran, D., Karkera, R., Durairai G, and Kumar S. 2023. *In-vitro* antibacterial activity of *Cnidoscolus chayamansa* leaves extract on selective bacterial strain . World Journal of Pharmacy and Pharmaceutical Sciences. doi: 10.20959/wjpps202310-25786

Fois, B., Skok, Ž., Tomašič, T., Ilaš, J., Zidar, N., Zega, A., Peterlin Mašič, L., Szili, P., Draskovits, G., Nyerges, A., Pál, C., and Kikelj, D. 2020. Dual E*scherichia coli* DNA gyrase A and B inhibitors with antibacterial activity. ChemMedChem, 15(3), 265-269. doi: 10.1002/cmdc.201900607

Fu, X., Belwal, T., Cravotto, G., and Luo, Z. 2020. Sono-physical and sono-chemical effects of ultrasound: Primary applications in extraction and freezing operations and influence on food components. Ultrasonics Sonochemistry. 60:104726. doi:10.1016/j.ultsonch.2019.104726

Fukumoto, L.R., and Mazza, G. 2000. Assessing antioxidant and prooxidant activities of phenolic compounds. Journal of Agricultural and Food Chemistry. 48(8):3597-3604. https://doi.org/10.1021/jf000220w

Garcia, C., and Blesso, C. N. 2021. Antioxidant properties of anthocyanins and their mechanism of action in atherosclerosis. Free Radical Biology and Medicine, 172, 152-166. doi: 10.1016/j.freeradbiomed.2021.05.040

Gutiérrez-Rebolledo, G.A., Pérez-González, M.Z., and Jiménez-Arellanes, M.A. 2016. Importancia nutricional, farmacológica y química de la chaya (*Cnidoscolus chayamansa*). Revisión bibliográfica. Revista de Temas Ciencia y Tecnologia. 20(60):43-56.

Guzmán, E.L., González, J.C.C., Flores, M.C., Carrillo, A.S., Pescador, M.G.N., and Cruz F.J.M. 2020. Effect on hyperglycemia and pancreas cells of chaya aqueous extracts from two different regions in streptozotocin-induced diabetes rats. Brazilian Journal of Pharmaceutical Sciences 56:1-5. doi: 10.1590/S2175-97902019000418782

Hanwell, M., Curtis, D., Lonie, D., Vandermeerschd, T., Zurek, E., and Hutchison, G. 2012. Avogadro: An advanced semantic chemical editor, visualization, and analysis platform. Journal of Cheminformatics. 1-17, 4(8).

Hartmann, M., and Lindhorst, T.K. 2011. The bacterial lectin FimH, a target for drug discovery–carbohydrate inhibitors of type 1 fimbriae-mediated bacterial adhesion. European Journal of Organic Chemistry (20-21), 3583-3609. https://doi.org/10.1002/ejoc.201100407

He, J., Qiao, W., An, Q., Yang, T., and Luo, Y. 2020. Dihydrofolate reductase inhibitors for use as antimicrobial agents. European Journal of Medicinal Chemistry. 195, 112268. doi: 10.1016/j.ejmech.2020.112268

Hazafa, A., Rehman, K.U., Jahan, N., and Jabeen, Z. 2020. The role of polyphenol (flavonoids) compounds in the treatment of cancer cells. Nutrition and Cancer. 72(3):386-397. doi: 10.1080/01635581.2019.1637006

Herrera-Pool, E., Ramos-Díaz, A.L., Lizardi-Jiménez, M. A., Pech-Cohuo, S., Ayora-Talavera, T., Cuevas-Bernardino, J.C., García-Cruz, U., and Pacheco, N. 2021. Effect of solvent polarity on the ultrasound assisted extraction and antioxidant activity of phenolic compounds from habanero pepper leaves (*Capsicum chinense*) and its identification by UPLC-PDA-ESI-MS/MS. Ultrasonics Sonochemistry, 76, 1-12. doi: 10.1016/j.ultsonch.2021.105658

Huang, D.D., Shi, G., Jiang, Y., Yao, C., and Zhu, C. 2020. A review on the potential of Resveratrol in prevention and therapy of diabetes and diabetic complications. Biomedicine & Pharmacotherapy, 125, 109767. doi: 10.1016/j.biopha.2019.109767

Hussain, Z., Khan, J.A., Arshad, M.I., Muhammad, F., and Abbas, R.Z. 2021. Comparative characterization of cinnamon, cinnamaldehyde and kaempferol for phytochemical, antioxidant and pharmacological properties using acetaminophen-induced oxidative stress mouse model. Boletin Latinoamericano y del Caribe Plantas Medicinales y Aromaticas. 20(4):339-350. doi: 10.37360/blacpma.21.20.4.25

Jug, G., Anderluh, M., and Tomašič, T. 2015. Comparative evaluation of several docking tools for docking small molecule ligands to DC-SIGN. Journal of Molecular Modeling. 21, 1-12 doi: 10.1007/s00894-015-2713-2

Kaabi, Y.A. 2022. Potential roles of anti-inflammatory plant-derived bioactive compounds: Targeting inflammation in microvascular complications of diabetes. Molecules. 27(21):7352. doi: 10.3390/molecules27217352.

Kahlon, A.K., Roy, S., and Sharma, A. 2010. Molecular docking studies to map the binding site of squalene synthase inhibitors on dehydrosqualene synthase of *Staphylococcus aureus*. Journal of Biomolecular Structure and Dynamics. 28(2), 201-210. doi: 10.1080/07391102.2010.10507353

Kuri-García, A., Godínez-Santillán, R. I., Mejía, C., Ferriz-Martínez, R. A., García-Solís, P., Enríquez-Vázquez, A., García-Gasca T., Guzmán-Maldonado S.H., and Chávez-Servín, J. L. 2019. Preventive effect of an infusion of the aqueous extract of Chaya leaves (*Cnidoscolus aconitifolius*) in an aberrant crypt foci rat model induced by azoxymethane and dextran sulfate sodium. Journal of medicinal food, 22(8), 851-860. doi: 10.1089/jmf.2019.0031

Laskowski, R.A., and Swindells, M.B. 2011. LigPlot+: multiple ligand-protein interaction diagrams for drug discovery. Journal of Chemical Information and Modeling. 51, 2778-2786. doi: 10.1021/ci200227u

Li, H., Han, J., Zhao, H., Liu, X., Ma, L., Sun, C., Yin, H., and Shi, Y. 2018. Investigation of the intermolecular hydrogen bonding effects on the intramolecular charge transfer process of coumarin 340 in tetrahydrofuran solvent. Journal of Cluster Science. 29(4):585-592. doi:10.1007/s10876-018-1371-9.

Liu, X., Ji, D., Cui, X., Zhang, Z., Li, B., Xu, Y., Chen, T., and Tian, S. 2020. p-Coumaric acid induces antioxidant capacity and defense responses of sweet cherry fruit to fungal pathogens. Postharvest Biology and Technology. 169:111297. doi:10.1016/j.postharvbio.2020.111297.

Magala, P., Klevit, R.E., Thomas, W.E., Sokurenko, E.V., and Stenkamp, R.E. 2020. RMSD analysis of structures of the bacterial protein FimH identifies five conformations of its lectin domain. Proteins 88(4), 593-603.M DOI: 10.1002/prot.25840

Ouadi, Y.E., Bendaif, H., Mrabti, H.N., Elmsellem, H., Kadmi, Y., Shariati, M.A., Abdel-Rahman, I., Hammouti, B., and Bouyanzer, A. 2017. Antioxidant activity of phenols and flavonoids contents of aqueous extract of *Pelargonium graveolens* orgin in the North-East Morocco. Journal of Microbiology Biotechnology and Food Sciences. 6(5):1218-1220. doi:10.15414/jmbfs.2017.6.5.1218-1220.

Pettersen, E.F., Goddard, T.D., Huang, C.C., Couch, G.S., Greenblatt, D.M., Meng, E.C., and Ferrin, T.E. 2004. UCSF Chimera--a visual-ization system for exploratory research and analysis. Journal of Computational Chemistry. 25(13):1605-1612. DOI: 10.1002/jcc.20084

Pérez-González, M.Z., Macías-Rubalcava, M.L., Hernández-Ortega, S., Siordia-Reyes, A.G., Jiménez-and Arellanes, M.A. 2019. Additional compounds and the therapeutic potential of *Cnidoscolus chayamansa* (McVaugh) against hepatotoxicity induced by antitubercular drugs. Biomedicine & Pharmacotherapy 117:1-10. doi:10.1016/j.biopha.2019.109140.

Pisoschi, A.M., Pop, A., Iordache, F., Stanca, L., Predoi, G., and Serban, A.I. 2021. Oxidative stress mitigation by antioxidants-an overview on their chemistry and influences on health status. European Journal of Medicinal Chemistry, 209, 112891. doi: 10.1016/j.ejmech.2020.112891.

Reuter, S., Gupta, S.C., Chaturvedi, M.M., and Aggarwal, B.B. 2010. Oxidative stress, inflammation, and cancer: How are they linked? Free Radical Biology and Medicine. 49(11):1603-1616. doi:10.1016/j.freeradbiomed.2010.09.006.

Rodrigues, M.M.R., Ojeda, J.C.M., Díaz, M.G., and Allende DKB. 2021. Use of chaya (*Cnidoscolus chayamansa*) leaves for nutritional compounds production for human consumption. The Journal of the Mexican Chemical Society. 65:118-128. doi:10.29356/jmcs.v65i1.1433.

Ruiz, J.C.R., Ordoñez, Y.B.M., Basto, Á.M., and Campos, M.R.S. 2015. Antioxidant capacity of leaf extracts from two S*tevia rebaudiana* Bertoni varieties adapted to cultivation in Mexico. Nutrición Hospitalaria. 31(3):1163-1170. doi:10.3305/nh.2015.31.3.8043.

Saiga, A., Tanabe, S., and Nishimura, T. 2003. Antioxidant activity of peptides obtained from porcine myofibrillar proteins by protease treatment. Journal of Agricultural and Food Chemistry. 51(12):3661-3667. doi:10.1021/jf021156g

Sissi, C., Vazquez, E., Chemello, A., Mitchenall, L.A., Maxwell, A., and Palumbo, M. 2010. Mapping simocyclinone D8 interaction with DNA gyrase: evidence for a new binding site on GyrB. Antimicrobial Agents and Chemotherapy. 54(1), 213-22S DOI: 10.1128/AAC.00972-09

Sudha, G., Priya, M.S., Shree, R.I., and Vadivukkarasi, S. 2011. *In vitro* free radical scavenging activity of raw pepino fruit (*Solanum muricatum aiton*). International Journal of Current Pharmaceutical Research. 3(2):137-140.

Tang, S., Chen, S., Tan, X., Xu, M., and Xu, X. 2022. Network pharmacology prediction and molecular docking-based strategy to explore the pharmacodynamic substances and mechanism of "Mung Bean" against bacterial infection. Drug Development and Industrial Pharmacy, 48(2), 58-68.

Us-Medina, U., Millán-Linares, M.D.C., Arana-Argaes E., and Segura-Campos, M.R. 2020. In vitro antioxidant and anti-inflammatory activity of Chaya extracts (*Cnidoscolus aconitifolius* (Mill.) IM Johnst). Nutricion Hospitalaria, 37(1), 46-55.

Vazquez-Armenta, F.J., Leyva, J.M., Mata-Haro, V., Gonzalez-Aguilar, G.A, Cruz-Valenzuela, M.R., Esqueda, M., Gutierrez, A., Nazzaro, F., Fratianni, F., Gaitan-Hernandez, R., and Ayala-Zavala, J.F. 2022. Phenolic compounds of *Phellinus* spp. with antibacterial and antiviral activities. Brazilian Journal of Microbiology, 53(3), 1187-1197. doi:10.1007/s42770-022-00745-x

Waterhouse, A., Bertoni, M., Bienert, S., Studer, G., Tauriello, G., Gumienny, R., Heer, F.T., de Beer, T.A.P., Rempfer, C., Bordoli, L., Lepore, R., Schwede, T. 2018. SWISS-MODEL: homology modelling of protein structures and complexes. Nucleic Acids Research. 46, W296-W303.

Wu, S.C., Liu, F., Zhu, K., and Shen, J. Z. 2019. Natural products that target virulence factors in antibiotic-resistant *Staphylococcus aureus*. Journal of Agricultural and Food Chemistry, 67(48), 13195-13211.